

# **IEICE** **TRANSACTIONS**

## **on Fundamentals of Electronics, Communications and Computer Sciences**

DOI:10.1587/transfun.2024EAP1081

Publicized:2024/12/09

This advance publication article will be replaced by  
the finalized version after proofreading.



A PUBLICATION OF THE ENGINEERING SCIENCES SOCIETY

The Institute of Electronics, Information and Communication Engineers

Kikai-Shinko-Kaikan Bldg., 5-8, Shibakoen 3 chome, Minato-ku, TOKYO, 105-0011 JAPAN

# Service Priority-Based Dynamic TDMA Protocol for FANETs

Siwei Yang<sup>†</sup>, Tingli Li<sup>†</sup>, Tao Hu<sup>†a)</sup>, Wenzhi Zhao<sup>†</sup>, Nonmembers

**SUMMARY** With the increasing number of tasks undertaken by unmanned aerial vehicle (UAV) clusters, the corresponding flight ad hoc networks must process an increasing amount of service data, and different service types have different transmission requirements. According to these requirements, existing methods often prioritize high-priority packets at the expense of low-priority packets. To overcome this limitation, this paper proposes a dynamic time-division multiple access (TDMA) protocol based on service priority called the SPD-TDMA protocol. To meet the requirements of packet transmission with different priorities, a queue-scheduling algorithm based on maximum waiting time was designed. In this algorithm, packets received from upper-layer applications are allocated to different queues according to their priority, and a corresponding waiting time step is allocated to each queue. Packets with higher priority have shorter waiting times. When the transmission time slot arrives, the packets with the shortest remaining waiting time are sent preferentially, which not only meets the transmission requirements of high-priority packets but also effectively avoids the starvation of low-priority packets. On this basis, to optimize the usage of time-slot resources further, the SPD-TDMA protocol adopts a priority predictive time-slot scheduling mechanism to avoid overbooking time slots or wasting idle time-slot resources to improve the overall efficiency and throughput of the network. Simulation results based on OMNeT++ indicated that compared with the IEEE 802.11DCF, TDMA, and P-TDMA protocols, the proposed method increases the packet delivery rate by 80%, 58%, and 27%, and throughput by 85%, 58%, and 29%, respectively.

**key words:** FANET, TDMA, queue scheduling, estimated time slot.

## 1. Introduction

With the rapid development of mobile communication technology, the flight ad hoc network (FANET) has demonstrated its unique and powerful role in civil and military fields. For disaster relief [1], environmental monitoring [2], and complex military reconnaissance and strike missions [3], the FANET provides unprecedented flexibility and efficiency, greatly expanding the range of applications of mobile communications technology. With the continuous expansion of application scenarios, the requirements for data transmission have become increasingly diversified, introducing new challenges into the design of media access control (MAC) protocols. For instance, emergency rescue scenarios require low latency and high reliability [4], while environmental monitoring emphasizes data integrity [5]. Consequently, existing research often categorizes tasks based on different priorities of service requirements: tasks requiring low latency and high reliability, such as emergency alarms, video surveillance, and real-time image transmission, are

classified as high-priority services, whereas tasks with higher tolerance for latency, such as status reports, log transmissions, and non-real-time sensor data, are considered low-priority services. Moreover, wireless resources in FANETs are limited. Maximizing channel utilization while ensuring high-priority services remains a significant challenge. High node density and mobility also require the MAC protocol to dynamically adapt to changes in network conditions. Additionally, the high mobility of nodes and frequent changes in topology make it difficult for traditional MAC protocols to adapt, necessitating the design of protocols that can be dynamically adjusted.

Currently, MAC protocols can be classified into two main types: competitive and distributive. A typical representative of competitive protocols is IEEE 802.11DCF, which primarily controls packet collisions through the CSMA/CA mechanism. In this mechanism, nodes listen to the channel before transmitting data and use a random backoff time to reduce the probability of simultaneous transmissions. Additionally, it uses the RTS/CTS mechanism to reserve the channel and employs an exponential backoff strategy when collisions are detected, further reducing the likelihood of collisions. This was also the first MAC standard introduced into FANET research [6]. In contrast, distributive protocols such as time division multiple access (TDMA) provide multi-node shared channels by allocating time slots, thereby reducing packet conflicts. In cases with a small amount of data, the performance of distributive protocols is often inferior to that of competitive protocols as a result of low slot utilization. However, with an increase in data flow at the application layer, the performance of competitive protocols may decrease due to increases in the packet collision probability, whereas the performance of distributive protocols is enhanced by an increase in slot utilization. Therefore, in data-intensive network environments, researchers often employ dynamic slot allocation. In dynamic slot allocation protocols, improving slot utilization has been the core focus of previous research. To reduce slot conflicts during data transmission, Borgonovo et al. [7] allowed nodes to reserve slots based on the frame load information of their neighbors. Lu et al. [8] introduced switching frames into a superframe structure and adopted adaptive switching technology for the main time slot to optimize the allocation sequence of network time slots. To reduce slot allocation conflicts, Jiang et al. [9] designed a collision-free MAC protocol based on carrier sensing. Expanding upon this approach, Yi et al. [10] introduced an idle slot reservation mechanism into allocated slots, which significantly improved the slot utilization rate. Considering

<sup>†</sup>The authors are with the School of Data and Target Engineering PLA Strategic Support Force Information Engineering University, Zhengzhou 450001, China.

a) E-mail: hutaengineering@163.com

the impact of node load on the performance of the network, Fu et al. [11] and Wang et al. [12] proposed load sensing and slot allocation strategies based on the grey correlation analysis method and proportion of node-sending queue usage, respectively, effectively balancing the network load. For large-scale networking scenarios, Liu et al. [13] adopted clustering technology to enable nodes to occupy resources dynamically according to service intensity through a dynamic TDMA protocol and realized cross-cluster communication through gateway nodes. In the study of dynamic time-slot allocation protocols, in addition to improving time-slot utilization, some researchers have conducted in-depth analyses and discussions on the challenges faced by networks in terms of adapting to different quality of service requirements for data transmission. Yang et al. [14] introduced an intent-driven network into the FANET to realize self-analysis and configuration based on traffic intent. Zhao et al. [15] introduced a node priority judgment mechanism, allowing nodes to have different access channels according to their own characteristics or the characteristics of the transmission services. Ye et al. [16] also considered service priority as a key parameter of time-slot allocation and optimized the frame structure by designing an improved distributed color constraint heuristic algorithm, thereby improving the time-slot utilization efficiency of the entire network system. Wu et al. [17] designed a priority preemption mechanism to ensure that service packages with a higher priority can be transmitted first. Based on the above discussion of existing dynamic slot allocation protocols, the following problems were identified:

- (1) Slot resources may be over-reserved by high-priority nodes, resulting in a waste of slot resources.
- (2) Allocation is often performed at the expense of low-priority packet transmission to meet the transmission requirements of high-priority nodes.

To solve these problems, this paper proposes a dynamic TDMA protocol based on service priorities called SPD-TDMA. To optimize the use of time-slot resources, each node estimates its required number of time slots according to its current priority, time-slot reservation status, and node priority in the previous frame before scheduling a time slot. The goal of this approach is to avoid the excessive occupation of time-slot resources by nodes with higher priorities. Additionally, to prevent low-priority packets from starving because they have not been sent for a long time, the system assigns an initial maximum waiting time step to each received packet, which depends on the priority of the packet. The higher the priority, the shorter the maximum waiting time step. However, with the passage of waiting time, the sending priority of low-priority packets increases correspondingly to ensure the fairness and efficiency of the network. In the SPD-TDMA protocol, each node dynamically adjusts its priority at the beginning of each frame by evaluating the remaining waiting time steps of packets with different priorities. Then, the node estimates the number of required reservations based on the slot

reservation number of the previous frame and node priority and reduces the slot conflict probability within two hops through bidirectional slot reservation information exchange between nodes to achieve fairer and more efficient network resource allocation. In the data transmission stage, nodes preferentially process packets with short remaining waiting time steps, which not only meets the transmission requirements of high-priority packets but also effectively prevents the starvation of low-priority packets. The main contributions of this study are as follows:

- (1) Adopting the quadratic exponential smoothing prediction method: optimizing time slot reservation to prevent over-reservation.
- (2) Introducing the maximum waiting time step mechanism: evaluating the priority of data packets to avoid the “starvation” phenomenon of low-priority data packets.

The remainder of this paper is organized as follows: Section 2 discusses the implementation mechanisms of the SPD-TDMA protocol in detail. Section 3 presents experimental results. Section 4 summarizes our findings and discusses future research directions.

## 2. SPD-TDMA protocol

To improve the utilization efficiency of time slot resources, this section explains the proposed dynamic TDMA protocol. Its frame structure and flowchart are shown in Figures 1 and 2, respectively. A complete protocol frame is composed of three subframes: the Claim subframe, the Response subframe, and the Info subframe. When the MAC layer receives a data packet from the upper layer, it first inserts the packet into the appropriate queue based on its priority. At the beginning of each frame, every node updates the remaining wait time steps for all buffered packets. Based on this, the node’s priority is calculated, and the number of time slots that can be reserved for this frame is estimated. In the Claim phase, each node in the network reserves communication time slots according to its own load situation. Next, during the Response phase, these reserved time slots are confirmed, and data packets meeting the transmission conditions are moved to the forwarding queue. Finally, in the Info phase, data packets are sent when the reserved time slot arrives. To address the time synchronization issue, this study adopts the TPSN synchronization algorithm, allowing for a maximum synchronization error of 20  $\mu$ s while still maintaining normal operation of the protocol.

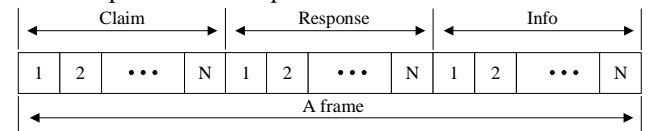


Fig. 1 Frame structure of SPD-TDMA.

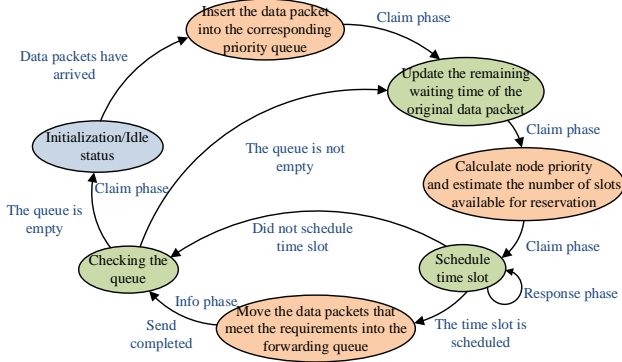


Fig. 2 SPD-TDMA protocol flowchart.

## 2.1 Scheduling algorithm based on a maximum-waiting-time queue

Although the statistical priority-based multiple access (SPMA) protocol provides a fine-grained priority scheduling mechanism, low-priority packets may experience excessive growth in service latency under a high network load. This can lead to a decrease in overall network efficiency, as low-priority tasks may be continually delayed, affecting the full utilization of network resources and response times.

Referring to the multi-priority mechanism of the SPMA protocol, Figure 3 shows four cache queues labeled 1, 2, 3, and 4, with priorities decreasing in turn. Each data packet is identified by two numbers: the number in the upper left corner represents the remaining waiting time step of the data packet, and the number in the lower right corner represents the order in which the data packet enters the node's cache queue. When the incoming upper-layer data packet reaches the MAC layer, it will be assigned to the corresponding queue based on its urgency and be given a maximum waiting time step  $t_{max_i}$ . The length of the time step is specified as the frame duration. For queue management, we adopt a hierarchical strategy where the  $t_{max_i}$  values corresponding to queues with lower priority are extended appropriately to ensure that packets with higher priority are processed first. However, over time, the sending priority of low-priority packets will gradually increase, which effectively mitigates the starvation phenomenon caused by long waiting times and achieves more balanced and efficient data transmission. At the beginning of each frame, the node updates the waiting time for the packets in its cache. If the time step of a packet drops to zero after subtracting the time step, then the packet must be sent immediately in the current frame. Therefore, packets that still have a remaining waiting time step (that does not fall to zero) must be temporarily placed to allow transmission opportunities and ensure that more time-sensitive packets are sent first. After completing the sending slot reservation phase, each node verifies the number of obtained slots. If at least one time slot is obtained, each node polls based on the remaining waiting time step level of the

packets in its cache and selects and moves the packets that meet the sending conditions to the forwarding queue for sending in the allocated time slot. If a node  $i$  reserves five time slots in the current frame, then the packets with packet numbers of  $i = 6, 3, 1, 2, 4$  will be transferred to the forwarding queue according to the specified order and will be sent successively in their allocated time slots. Similarly, if node  $i$  acquires eight slots, then it places packets with packet numbers of  $i = 6, 3, 1, 2, 4, 5, 10, 13$  in the forwarding queue to be transmitted in the corresponding slots.

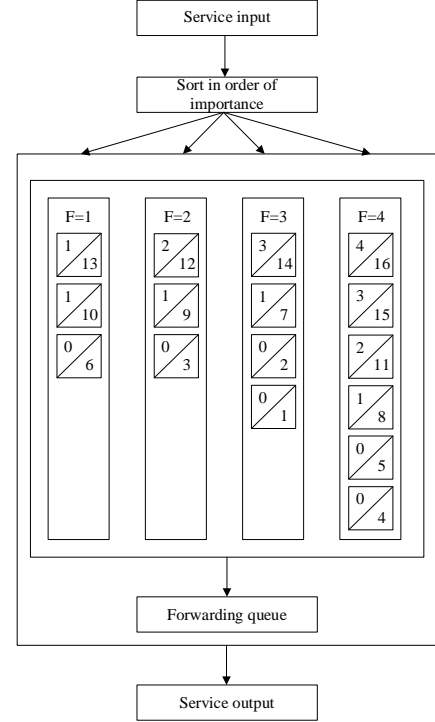


Fig. 3 Single-node congestion model.

## 2.2 Claim phase

In the Claim phase, if a node's cache queue is not empty, the node attempts to reserve a slot when its allocated slot arrives. First, the node calculates the priority  $W_t$  based on its own load as follows:

$$W_t = \omega_1 N_{wait0} + \omega_2 N_{wait1} + \omega_3 N_{wait2} + \omega_4 N_{wait3} + \omega_5 N_{wait4}, \quad (1)$$

where  $N_{waiti}$  represents the total number of packets whose remaining waiting time step is  $i$ , and  $\omega_i$  denotes the weighting factors corresponding to such packets.

Based on the calculated priority weight  $W_t$ , the node next estimates the number of slots it can reserve in the current network state  $NS_t$ . When a node performs slot reservation for the first time, it is assumed that the number of packets in its queue corresponds to the expected number of slots that can be reserved. However, for subsequent appointments,

nodes utilize historical appointment data to perform more precise predictions based on a quadratic exponential smoothing algorithm. Quadratic exponential smoothing is a forecasting technique that improves prediction accuracy by giving more recent observations more weight. The specific steps are as follows:

(1) Calculate the actual ratio of the previous frame  $R_{t-1}$ , which is the ratio of the final available slot number  $NS_{t-1}$  of the node in the previous frame to the calculated node priority  $W_{t-1}$ .

$$R_{t-1} = \frac{NS_{t-1}}{W_{t-1}} \quad (2)$$

(2) Calculate the first and second exponential smoothing values  $S_t^{(1)}$  and  $S_t^{(2)}$  based on the corresponding ratios. These smoothing values are calculated by combining the smoothing values of the previous time steps ( $S_{t-1}^{(1)}$  and  $S_{t-1}^{(2)}$ ) with  $R_{t-1}$  as follows:

$$S_t^{(1)} = \alpha \times R_{t-1} + (1 - \alpha) \times S_{t-1}^{(1)}, \quad (3)$$

$$S_t^{(2)} = \alpha \times S_t^{(1)} + (1 - \alpha) \times S_{t-1}^{(2)}, \quad (4)$$

where  $\alpha$  is an exponential smoothing coefficient and with a value range of  $(0,1)$ . The larger the value of  $\alpha$ , the larger the component of the data that is close to the predicted state.

(3) The node uses the following formulas to determine the required parameter  $a_t$  and trend term  $b_t$  for linear extrapolation, and obtain the predicted ratio  $R_t$  of the current time step:

$$a_t = 2S_t^{(1)} - S_t^{(2)}, \quad (5)$$

$$b_t = \frac{\alpha}{(1 - \alpha)} (S_t^{(1)} - S_t^{(2)}), \quad (6)$$

$$R_t = a_t + b_t. \quad (7)$$

(4) The expected number of reserved slots  $NS_t$  of a node is calculated by multiplying the predicted ratio  $R_t$  of the current time step by the weight  $W_t$  of the current priority.

$$NS_t = R_t * W_t \quad (8)$$

After prediction is complete, the node determines its slot reservation based on the number of predicted slots. The node listens to the time-slot reservation request information sent by neighboring nodes in the previous time slot and selects time slots that have not been reserved. If the number of free slots does not meet the demand, a node may consider preempting the slots reserved by nodes with a lower priority. After the reservation is complete, the node notifies neighboring nodes of the current slot reservation via

broadcasting.

When a node receives slot reservation information from a neighboring node while listening, it compares the received information with the information it already knows. If there is a conflict (i.e., different nodes try to reserve the same time slot), then the node with a higher priority weight will be given the right to use that time slot, whereas the node with a lower priority will choose another unreserved time slot or wait for the next frame.

### 2.3 Response phase

In the Response phase, each node in the network broadcasts its time-slot reservation information to its neighbors in the allocated time slot. In other time slots, the nodes adjust their time-slot arrangement according to the time-slot reservation information received from their neighbors. After this phase is completed, each node checks the slot reservation status and migrates packets that meet the transmission requirements to the forwarding queue based on the number of slot reservations. Additionally, if there are still unreserved time slots, then the average number of time slots that can be reserved for these nodes is calculated, which is combined with the number of time slots reserved for nodes to determine the maximum number of time slots that can be reserved for a node in the current frame. This value is then used by the node in the next frame to estimate the number of reserved slots.

### 2.4 Info phase

In the Info phase, the node sends packets to the forwarding queue in its own scheduled time slot, and for the remainder of the time, the node is in the receiving mode and ready to accept packets that may come from other nodes. When a new frame arrives, each node enters the Claim phase again and begins to reassign and reserve new time slots to ensure the continuous transmission and reception of data.

## 3. Simulation experiments and performance analysis

In this section, the OMNeT++ network simulator is used to compare the performance of the proposed SPD-TDMA protocol with that of the TDMA and P-TDMA protocols. Regarding computational complexity, TDMA is  $O(n)$ , P-TDMA is  $O(n^3)$ , and the SPD-TDMA includes a scenario where, in the event of a slot reservation conflict, nodes with lower priority explore the possibility of unreserved slots. This additional processing step increases the complexity of SPD-TDMA to  $O(n^4)$ . Through this comparison, the performance of the SPD-TDMA protocol can be effectively evaluated in terms of real-time adjustment of slot allocation, improvement of transmission efficiency and stability under the condition of higher computational complexity. In our simulation experiments, a multi-hop clustering algorithm inspired by Physaloides polycephalus was adopted in the

network layer to divide the UAV cluster into multiple subgroups [18]. An inter-cluster routing protocol based on the hybrid ant colony algorithm was adopted for this clustering structure to plan and maintain the transmission path. Additionally, the service packets generated by the application layer are divided into three categories, and the control packets of the network layer are considered. In the scheduling queue, the priorities are as follows: service 1, service 2, control, and service 3 packets, in descending order. The detailed simulation parameters are listed in Table 1.

**Table 1** Parameter settings for simulation experiments.

Simulation parameter	Parameter value
Clustering algorithm	PICA
Intercluster routing	ICRP
MAC protocol	IEEE 802.11 DCF, TDMA, P-TDMA, SPD-TDMA
Simulation time	120 s
Simulation scene size	1500 × 1500 m <sup>2</sup>
Number of nodes	40 to 80
Maximum speed	72 to 216 km/h
Communication distance	200 m
Moving model	Gauss-Markov movement model
Carrier frequency	2.4 GHz
Service 1 data stream	600 kbps
Service 2 data stream	600 kbps
Service 3 data stream	400 kbps
Starting energy	5 J

### 3.1 Average end-to-end delay

The average end-to-end delay represents the average time required for a packet to reach the destination node, and a low delay means that the protocol can process and transmit data quickly and efficiently, thereby reducing conflicts and waiting times. Figure 4 presents a performance comparison of the SPD-TDMA protocol with the IEEE 802.11DCF, TDMA, and P-TDMA protocols in terms of the average end-to-end delay at different maximum flight speeds. One can see that the average end-to-end delay is proportional to the flight speed of the UAV because an increase in the speed of the UAV will cause frequent link disconnection between the two points, which may indicate packet loss. Therefore, the retransmission mechanism is frequently enabled to attempt to resend packets, and the final packets will take longer to reach the destination node. Compared with the TDMA and P-TDMA protocols, the proposed SPD-TDMA protocol achieved a lower average end-to-end delay for all simulated bee colonies with maximum flight speeds, with average end-to-end delay reductions of 55% and 48%, respectively. This is because SPD-TDMA updates the node priority according to the node load in each frame and then makes slot reservations based on the estimated number of available slots. This reduces the waste of resources caused by overbooking time slots, thereby reducing the end-to-end delay. In contrast, the TDMA and P-TDMA protocols do not consider the actual transmission needs of nodes and their neighbors and set a fixed transmission slot or priority for each node. This approach can cause slot resources to be underutilized, which increases the average end-to-end delay.

However, the average end-to-end delay of the SPD-TDMA protocol was 78% higher than that of IEEE 802.11 DCF. The main reason for this increase in delay is the fixed slot reservation mechanism of the dynamic TDMA protocol, which leads to a certain delay in data transmission compared with the real-time channel competition of IEEE 802.11DCF. Figure 5 presents the average end-to-end delay of the three types of service packets in the SPD-TDMA protocol at different maximum flight speeds. When the node flight speed is low, the difference in the average end-to-end delay between the three types of service packets is insignificant. However, with an increase in the node flight speed, the average end-to-end delay gap between the three packet types gradually increases. This is because with an increase in flight speed, the success rate of data transmission between nodes decreases, resulting in an increase in the cached data packets of nodes. To ensure the transmission of high-priority data packets, the queuing time of low-priority data packets is increased, and the end-to-end delay gap between different service data packets gradually widens.

In UAV swarm communication, in addition to the impact of moving speed on communication, the number of nodes is crucial. Figure 6 shows that at a maximum moving speed of 20 m/s, the average end-to-end delay is proportional to the number of nodes. This is because the increase in the number of nodes leads to an increase in the packet collision frequency under the IEEE 802.11 DCF protocol. For the SPD-TDMA, TDMA, and P-TDMA protocols, as the number of nodes increases, the length of each frame also increases, and nodes require longer time to wait for their turn to send time slots, which increases the average delay of the entire system. Compared with the TDMA and P-TDMA protocols, the SPD-TDMA protocol reduces the average end-to-end delay by 50.4% and 49.5%, respectively. The reason is that the SPD-TDMA protocol improves the time slot utilization rate and makes communication more efficient. In Figure 7, as the number of nodes increases, the average delay gap of the three services continues to increase. Thus, in the case of increased congestion and competition, the SPD-TDMA protocol can ensure the transmission of high-priority data packets so that its delay remains low.

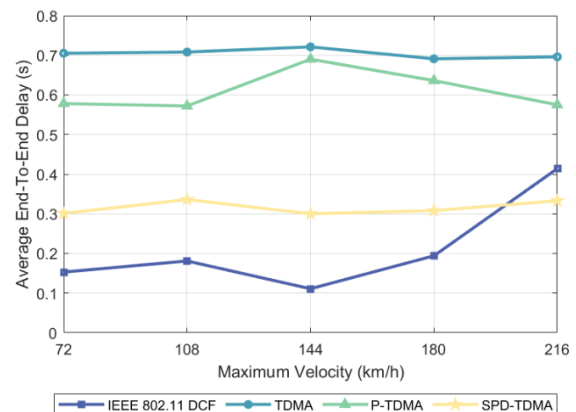


**Fig. 4** Performance comparison of average end-to-end delay at different maximum node speeds.

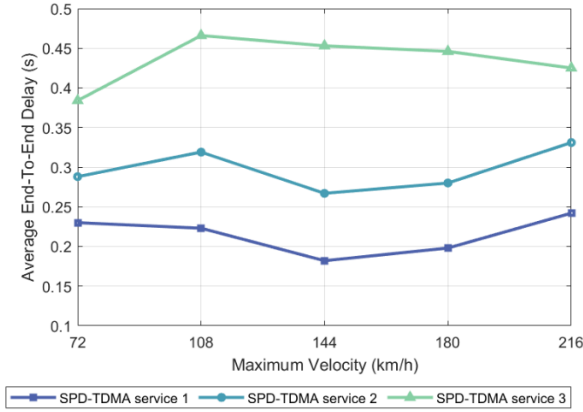


**Fig. 5** Performance comparison of the average end-to-end delay of different service packets at different maximum node speeds.

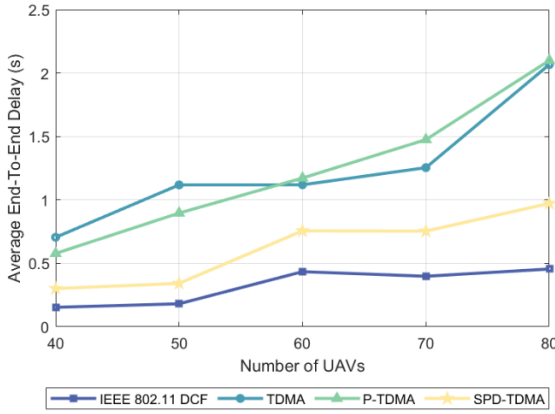


**Fig. 6** Performance comparison of the average end-to-end delay at different numbers of nodes.

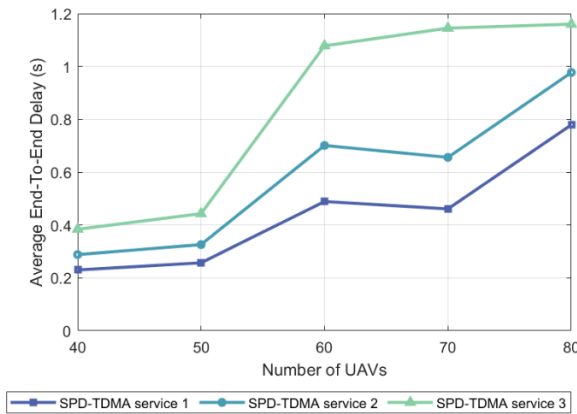


**Fig. 7** Performance comparison of the average end-to-end delay of

different service packets at different numbers of nodes.

### 3.2 Packet delivery rate

The packet delivery rate represents the proportion of successfully sent packets. A high packet delivery rate indicates that most packets can successfully reach their destination, demonstrating that the MAC protocol can effectively reduce data loss or errors, handle data conflicts in the network, and provide good error detection and recovery capabilities. Figure 8 presents the packet delivery performance of the SPD-TDMA protocol compared with that of the IEEE 802.11DCF, TDMA, and P-TDMA protocols at different maximum flight speeds. One can see that the packet delivery rate decreases with an increase in UAV flight speed because an increase in UAV speed increases the probability of link disconnection between two points, resulting in increased packet loss. Compared with the IEEE 802.11DCF, TDMA, and P-TDMA protocols, the proposed SPD-TDMA protocol provided a higher packet delivery rate for all simulated colonies with the highest flight speed, with packet delivery rate increases of 104%, 77%, and 43%, respectively. This is because in each frame, SPD-TDMA dynamically updates the node priority according to the node load and estimates the number of available slots according to the actual demand so that it can adjust the slot allocation more flexibly, avoid resource waste, and better meet the needs of inter-node transmission, thereby improving the packet delivery rate. In contrast, the TDMA and P-TDMA protocols do not consider the actual transmission needs of nodes and their neighbors and set a fixed transmission slot or priority for each node. Therefore, time-slot resources may not be fully utilized, which reduces the packet delivery rate. However, in IEEE 802.11DCF, the transmission of packets depends on the channel competition mechanism, and multiple nodes compete for channels simultaneously, which may lead to collisions and conflicts, negatively affecting the transmission rate of packets. In particular, in a large-data-flow scenario, competition becomes more intense, resulting in more collisions and retransmissions, which reduces the packet delivery rate. Figure 9 presents the packet delivery rates of the three types of service packets in the SPD-TDMA protocol at different maximum flight speeds. At different maximum flight speeds, the packet delivery rates of the three types of service packets are not significantly different. These results demonstrate that the SPD-TDMA protocol can dynamically adjust the priority of nodes, estimate available slots and reserve slots, and effectively balance the transmission requirements of different priority packets, preventing low-priority packets from being crowded out by high-priority packets.

Figure 10 illustrates that as the number of nodes increases, the packet delivery ratio of the four protocols generally decreases. This is primarily due to the increase in the number of nodes leading to an increase in the packet collision frequency of the IEEE 802.11 DCF protocol, which

increases the phenomenon of nodes discarding packets. For TDMA-like protocols, a longer frame delay may cause the node buffer to overflow more easily under high traffic conditions, resulting in packet loss and a decrease in the delivery ratio. Although the SPD-TDMA protocol increased the packet delivery ratio by 39.1% and 13.7%, respectively, compared to the TDMA and P-TDMA protocols, as the number of nodes increases, the delivery ratio of this protocol decreases the most. This indicates that in a high-load and high-complexity network environment, the complexity of the protocol will significantly affect performance. In Figure 11, although the delivery ratios of the three types of service packets all show a downward trend, the decline amplitudes are basically the same. This demonstrates that in the case of increased congestion and competition, although the protocol prioritizes sending high-priority service packets, through the maximum waiting time step mechanism, the protocol avoids excessively sacrificing the sending opportunities of low-priority service packets, thereby preventing a large number of them from being starved. Overall, this shows the relatively balanced scheduling ability of the protocol among different priority data packets.

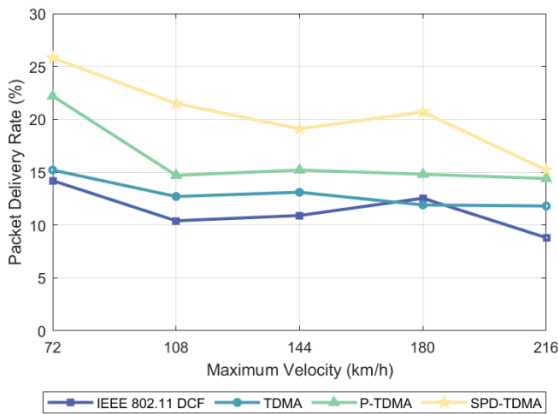


Fig. 8 Performance comparison of packet delivery rates at different maximum node speeds.

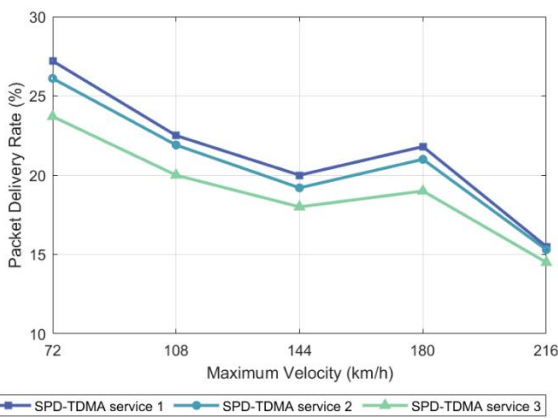


Fig. 9 Performance comparison of different service packet delivery rates at different maximum node speeds.

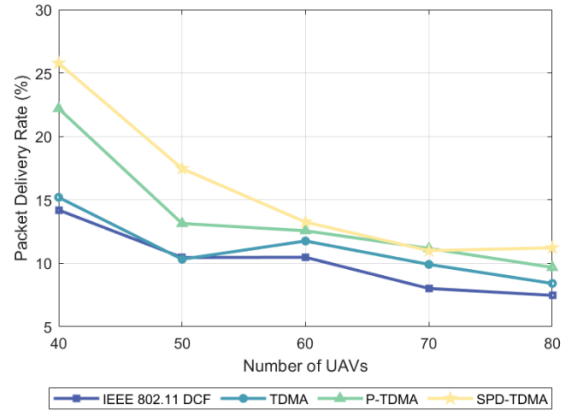


Fig. 10 Performance comparison of packet delivery rates at different numbers of nodes.

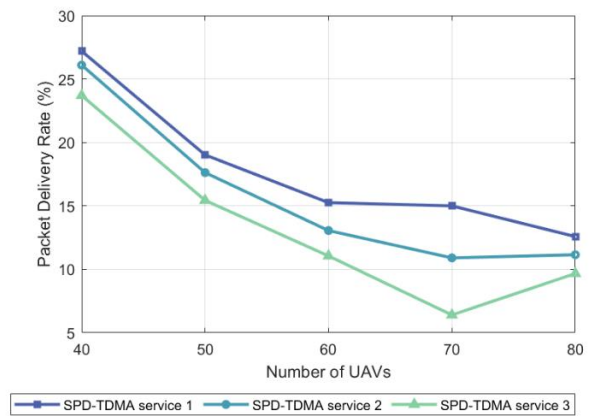


Fig. 11 Performance comparison of different service packet delivery rates at different numbers of nodes.

### 3.3 Throughput

Throughput is expressed as the number of packets successfully sent to a destination node in a given period. High throughput typically requires protocols that reduce idle and collision times, balance bandwidth allocation, and dynamically tune network performance. Figure 12 presents a throughput performance comparison of the SPD-TDMA protocol with the IEEE 802.11DCF, TDMA, and P-TDMA protocols at different maximum flight speeds. One can see that throughput is inversely proportional to the speed of UAVs because the quality of the channels between UAVs decreases as speed increases. This can lead to increased packet loss or retransmission during data transmission, which reduces the overall throughput. Additionally, as the flight speed increases, data packets may experience longer transmission delays. This can result in increased packet queuing for transmission in the same time period, thereby reducing the overall throughput. Compared with the IEEE

802.11DCF, TDMA, and P-TDMA protocols, the proposed SPD-TDMA protocol has higher throughput for all simulated swarms with maximum flight speeds, with throughput increases of 109%, 77%, and 45%, respectively. This is because, unlike the TDMA and P-TDMA protocols, SPD-TDMA considers the actual transmission requirements of nodes and their neighbors, avoids the setting of fixed transmission slots or priorities, and effectively improves the utilization of time-slot resources, thereby improving the overall throughput. In IEEE 802.11DCF, packet transmission is affected by the channel competition mechanism. Multiple nodes competing for channels simultaneously may lead to collisions and conflicts, which in turn affect the packet transmission rate. Particularly in the case of large data volumes, competition becomes more intense, increasing the risk of collision and retransmission and ultimately resulting in a lower overall throughput.

Figure 13 presents the throughput of the three different types of service packets in SPD-TDMA at different maximum flight speeds. As node movement speed increases, the differences between the throughput values of the three types of data packets do not increase, indicating that the SPD-TDMA protocol can effectively manage different types of data flows, maintain the consistency and robustness of data transmission, and adapt to the dynamic changes introduced by node movement.

Figure 14 shows that the throughput of four protocols is inversely proportional to the number of nodes. This is primarily because as the number of nodes increases, the packet collision frequency in the IEEE 802.11 DCF protocol increases, leading to network congestion and overall throughput reduction. For TDMA-like protocols, the increase in the number of nodes makes the longer frame delay more likely to cause node buffer overflow under high traffic conditions, thereby leading to packet loss and throughput reduction. In contrast, the SPD-TDMA protocol has a higher throughput. Compared with the IEEE 802.11 DCF, TDMA, and P-TDMA protocols, it increased by 54.6%, 40.7%, and 15.3%, respectively. This is because the SPD-TDMA protocol improves the time slot utilization rate. However, owing to the high complexity of this protocol, the performance degradation amplitude is also large. In practical applications, the SPD-TDMA protocol still has significant advantages. Figure 15 shows that the difference in packet throughput of three priority services does not increase with the increase in the number of nodes. Thus, this protocol has a relatively balanced scheduling ability among different priority data packets.

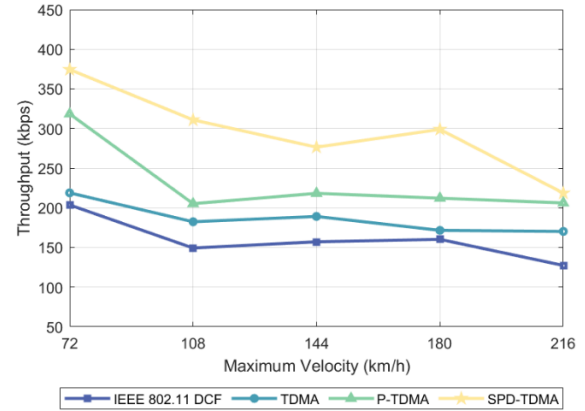


Fig. 12 Performance comparison of total throughput at different maximum node speeds.

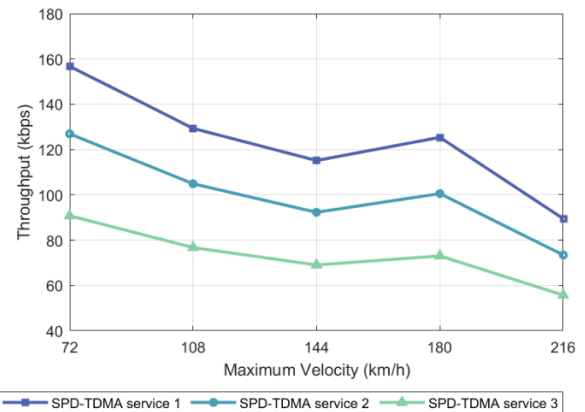


Fig. 13 Performance comparison of different service throughputs at different maximum node speeds.

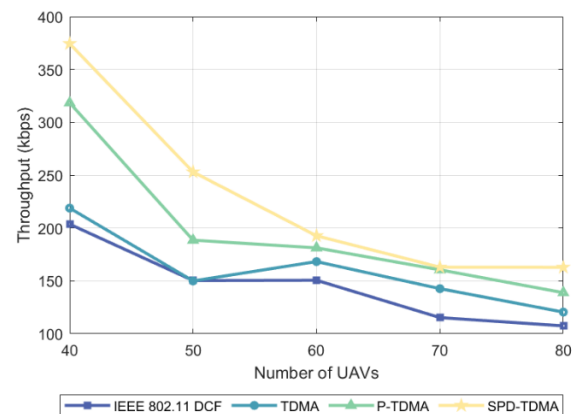


Fig. 14 Performance comparison of total throughput at different numbers of nodes.

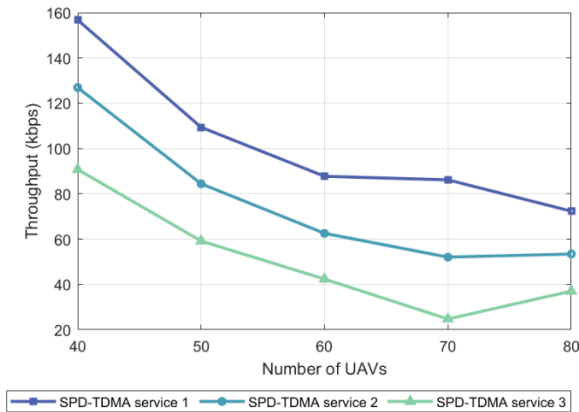


Fig. 15 Performance comparison of different service throughputs at different numbers of nodes.

#### 4. Conclusion

To address the problem of existing dynamic TDMA protocols not fully utilizing time-slot resources and sacrificing low-priority packet transmission requirements, this paper proposes a dynamic TDMA protocol based on service priority. In the time-slot reservation phase, the proposed protocol dynamically adjusts the node priority according to the data packets in the buffer to predict available time slots and make time-slot reservations to avoid excessive reservation or wasting of idle time-slot resources and improve the overall utilization efficiency of network resources. In the data transmission stage, by preferentially transmitting packets with smaller waiting times, the transmission requirements of high-priority packets are ensured, and the starvation of low-priority packets is effectively avoided. Experimental results demonstrated that the proposed dynamic TDMA protocol has excellent processing efficiency. Compared with the IEEE 802.11DCF, TDMA, and P-TDMA protocols, the proposed protocol increased the packet delivery rate by 80%, 58%, and 27%, respectively, and the throughput by 85%, 58%, and 29%, respectively. In future research, we will explore how to utilize heuristic algorithms to perform comprehensive scheduling across multiple dimensions, such as time, frequency, and space, to optimize network performance. Additionally, we recognize that under conditions of low signal-to-noise ratio, nodes may fail to successfully demodulate the slot reservation requests sent by neighboring nodes, which could affect the effectiveness of existing methods. We will introduce network coding technology in subsequent research to address this issue. Through network coding, nodes can reconstruct critical control data using redundant information in scenarios with poor signal-to-noise ratios, thereby enhancing the reliability and robustness of control information and ensuring stable network operation.

#### References

- [1] M. Silvagni, A. Tonoli, E. Zenerino, and M. Chiaberge, "Multipurpose UAV for search and rescue operations in mountain avalanche events," *Geomatics, Natural Hazards and Risk*, vol. 8, no. 1, pp. 18–33, Oct. 2016, doi: 10.1080/19475705.2016.1238852.
- [2] S. Asadzadeh, W. J. de Oliveira, and C. R. de Souza Filho, "UAV-based remote sensing for the petroleum industry and environmental monitoring: State-of-the-art and perspectives," *Journal of Petroleum Science and Engineering*, vol. 208, p. 109633, Jan. 2022, doi: 10.1016/j.petrol.2021.109633.
- [3] H. Deng, J. Huang, Q. Liu, T. Zhao, C. Zhou, and J. Gao, "A Distributed Collaborative Allocation Method of Reconnaissance and Strike Tasks for Heterogeneous UAVs," *Drones*, vol. 7, no. 2, p. 138, Feb. 2023, doi: 10.3390/drones7020138.
- [4] T. Ahn, J. Seok, I. Lee, and J. Han, "Reliable flying IoT networks for UAV disaster rescue operations," *Mobile Information Systems*, vol. 2018, pp. 1–12, 2018, doi: 10.1155/2018/2572460.
- [5] T. T. Sari, S. Ahmad, A. Aral, and G. Seçinti, "Collaborative smart environmental monitoring using flying edge intelligence," *GLOBECOM 2023-2023 IEEE Global Communications Conference*, vol. 7, pp. 5336–5341, Dec. 2023, doi: 10.1109/globecom54140.2023.10436927.
- [6] T. Brown, B. Argrow, C. Dixon, S. Doshi, R.-G. Thekkekkunnel, and D. Henkel, "Ad Hoc UAV Ground Network (AUGNet)," *AIAA 3rd "Unmanned Unlimited" Technical Conference, Workshop and Exhibit*, Jun. 2004, doi: 10.2514/6.2004-6321.
- [7] F. Borgonovo, A. Capone, M. Cesana, and L. Fratta, "RR-ALOHA, a Reliable R-ALOHA broadcast channel for ad-hoc inter-vehicle communication networks," *Proceedings of Med-Hoc-Net*, 2002.
- [8] Y. Lu, Z. Qiu, Y. Luo, L. Wei, S. Lin, and X. Liu, "A Modified TDMA Algorithm Based on Adaptive Timeslot Exchange in Ad Hoc Network," *2018 IEEE 4th International Conference on Computer and Communications (ICCC)*, Dec. 2018, doi: 10.1109/compcomm.2018.8780678.
- [9] A. Jiang, Z. Mi, C. Dong, and H. Wang, "CF-MAC: A collision-free MAC protocol for UAVs Ad-Hoc networks," *2016 IEEE Wireless Communications and Networking Conference*, Apr. 2016, doi: 10.1109/wcnc.2016.7564844.
- [10] Y. Lu, J. Fu, H. Qiu, J. Lin, and Y. Li, "Idle time slot reservation TDMA protocol for flying ad-hoc networks," *Computer Engineering*, vol. 47, no. 3, pp. 202–208, 2021, doi: 10.19678/j.issn.1000-3428.0057479.
- [11] Y. Fu, N. Zhang, J. Wei, S. Qu, Y. Lu, and C. Liu, "OPNET based simulation of hybrid TDMA protocol for helicopters datalink," *Journal of System Simulation*, vol. 34, no. 9, pp. 1933–1940, 2022.
- [12] M. Wang and H. Li, "NPB-DTDM: a node priority-based dynamic TDMA algorithm based on the usage proportion of sending queue," *5th International Conference on Information Science, Electrical, and Automation Engineering (ISEAE 2023)*, Aug. 2023, doi: 10.1117/12.2689836.
- [13] Q. Liu and W. Yuan, "Research on a media access control protocol of cluster-based MANET," *Journal of Beijing Jiaotong University*, vol. 42, no. 2, p. 54, 2018.
- [14] L. Yang et al., "Reservation and Traffic Intent-Aware Dynamic Resource Allocation for FANET," *2021 IEEE 21st International Conference on Communication Technology (ICCT)*, Oct. 2021, doi: 10.1109/icct52962.2021.9657907.
- [15] J. Zhao, S. Guo, and J. Yang, "A dynamic TDMA protocol for flying ad-hoc network applications," *Electronic Measurement Technology*, vol. 43, no. 23, pp. 133–138, 2020, doi:10.19651/j.cnki.emt.2005138.
- [16] Y. Ye, X. Zhang, L. Xie, and K. Qin, "A Dynamic TDMA Scheduling Strategy for MANETs Based on Service Priority," *Sensors*, vol. 20, no. 24, p. 7218, Dec. 2020, doi: 10.3390/s20247218.
- [17] G. Wu, C. Dong, A. Li, L. Zhang, and Q. Wu, "FM-MAC: A Multi-Channel MAC Protocol for FANETs with Directional Antenna,"

2018 IEEE Global Communications Conference (GLOBECOM), Dec. 2018, doi: 10.1109/glocom.2018.8648025.

[18] S. Yang, T. Li, D. Wu, T. Hu, W. Deng, and H. Gong, "Bio-inspired multi-hop clustering algorithm for FANET," *Ad Hoc Networks*, vol. 154, p. 103355, Mar. 2024, doi: 10.1016/j.adhoc.2023.103355.



**Siwei Yang** was born in 1999 in Anyang, Henan province. He is currently pursuing a master's degree at the School of Data and Target Engineering, PLA Strategic Support Force Information Engineering University. His research interest is flying ad hoc network.



**Tingli Li** was born in 1989 in Anyang, Henan province. He is an associate professor at the School of Data and Target Engineering, PLA Strategic Support Force Information Engineering University. His research interests include radar signal analysis and processing and early warning detection.



**Tao Hu** was born in 1976 in Tongcheng, Anhui province. He is a professor at the School of Data and Target Engineering, PLA Strategic Support Force Information Engineering University. His research interests include radar signal analysis and processing and early warning detection.



**Wenzhi Zhao** was born in 1998 in Zhengzhou, Henan province. He is currently pursuing a master's degree at the School of Data and Target Engineering, PLA Strategic Support Force Information Engineering University. His research interest is secure routing.

Fig. 7 Performance comparison of the average end-to-end delay of different service packets at different numbers of nodes.

Fig. 8 Performance comparison of packet delivery rates at different maximum node speeds.

Fig. 9 Performance comparison of different service packet delivery rates at different maximum node speeds.

Fig. 10 Performance comparison of packet delivery rates at different numbers of nodes.

Fig. 11 Performance comparison of different service packet delivery rates at different numbers of nodes.

Fig. 12 Performance comparison of total throughput at different maximum node speeds.

Fig. 13 Performance comparison of different service throughputs at different maximum node speeds.

Fig. 14 Performance comparison of total throughput at different numbers of nodes.

Fig. 15 Performance comparison of different service throughputs at different numbers of nodes.

### List of Captions

Table 1 Parameter settings for simulation experiments.

Fig. 1 Frame structure of SPD-TDMA.

Fig. 2 SPD-TDMA protocol flowchart.

Fig. 3 Single-node congestion model.

Fig. 4 Performance comparison of average end-to-end delay at different maximum node speeds.

Fig. 5 Performance comparison of the average end-to-end delay of different service packets at different maximum node speeds.

Fig. 6 Performance comparison of the average end-to-end delay at different numbers of nodes.